NANO LETTERS

Letter

Reversible Basal Plane Hydrogenation of Graphene

Sunmin Ryu, Melinda Y. Han, Janina Maultzsch, Tony F. Heinz, Philip Kim, Michael L. Steigerwald, and Louis E. Brus

Nano Lett., **2008**, 8 (12), 4597-4602 • DOI: 10.1021/nl802940s • Publication Date (Web): 18 November 2008

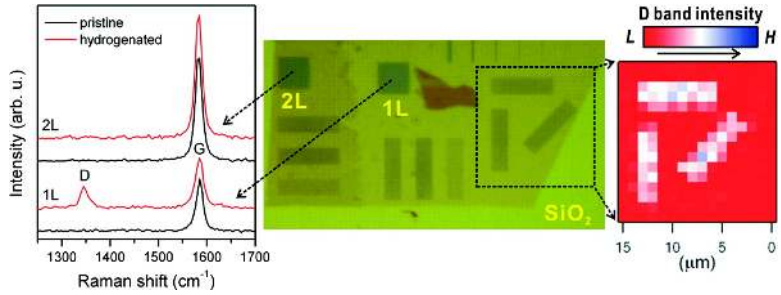

More About This Article

Additional resources and features associated with this article are available within the HTML version:

- Supporting Information
- Access to high resolution figures
- Links to articles and content related to this article
- Copyright permission to reproduce figures and/or text from this article

View the Full Text HTML

Nano Letters is published by the American Chemical Society. 1155 Sixteenth Street N.W., Washington, DC 20036

NANO LETTERS

2008
Vol. 8, No. 12
4597-4602

Reversible Basal Plane Hydrogenation of Graphene

Sunmin Ryu,[†] Melinda Y. Han,[‡] Janina Maultzsch,[§] Tony F. Heinz,[§] Philip Kim,[||] Michael L. Steigerwald, and Louis E. Brus*[,†]

Department of Chemistry, Department of Applied Physics and Applied Mathematics, Departments of Physics and Electrical Engineering, and Department of Physics, Columbia University, New York, New York 10027

Received September 26, 2008; Revised Manuscript Received November 3, 2008

ABSTRACT

We report the chemical reaction of single-layer graphene with hydrogen atoms, generated in situ by electron-induced dissociation of hydrogen silsesquioxane (HSQ). Hydrogenation, forming sp^3 C−H functionality on the basal plane of graphene, proceeds at a higher rate for single than for double layers, demonstrating the enhanced chemical reactivity of single sheet graphene. The net H atom sticking probability on single layers at 300 K is at least 0.03, which exceeds that of double layers by at least a factor of 15. Chemisorbed hydrogen atoms, which give rise to a prominent Raman D band, can be detached by thermal annealing at 100∼200 °C. The resulting dehydrogenated graphene is "activated" when photothermally heated it reversibly binds ambient oxygen, leading to hole doping of the graphene. This functionalization of graphene can be exploited to manipulate electronic and charge transport properties of graphene devices.

Graphene, a single atomic plane of graphite, has outstanding electronic and structural properties and is a promising candidate for nanoelectronic circuits.[1,2] With the availability of large-area graphene samples, the current top-down fabrication processes based on lithography may be extended to graphene-based devices. Also, thin graphene layers have been actively studied for applications as transparent electrodes and as nanocomposite materials.[3,4] The materials chemistry of single-sheet graphene has not yet been explored in detail,[5] and such knowledge is essential for its practical use in technology.

Multilayer graphite shows high in-plane strength due to aromatic bond conjugation, and the basal plane is relatively inert chemically. However, single-layer graphene is significantly more reactive with molecular O_2 than graphite.[6,7] This enhanced reactivity may result from the influence of structural distortion. Free-standing graphene at 23 °C shows spontaneous rippling of ∼1 nm magnitude and ∼10 nm wavelength.[8] In addition, fluctuating patterns of long−short bond alternation around individual C atoms are predicted.[9] Such structural elasticity[10] apparently enables graphene to conform to atomically rough substrates as seen in recent scanning tunneling microscopy studies on silicon dioxide.[11,12] The local strain built into the rippled, deformed graphene should stabilize transition states of chemical reactions requiring local sp^3 hybridization, as shown in the hydrogenation of C_{60} molecules, carbon nanotubes, and graphite.[13] It is well known that the curved surfaces of carbon nanotubes exhibit higher chemical reactivity than the planar sheets of graphene.[14]

In this letter, we use Raman spectroscopy to study the reaction of graphene with hydrogen atoms generated during electron beam initiated cross-linking of a hydrogen silsesquioxane (HSQ) film coated on the graphene sample. Graphene Raman scattering is sensitive to structure and doping[15] and does not require electrical contacts. We find the reaction to be significantly faster for single-layer graphene than for double layers. Also, we observe that hydrogenated graphene can be restored by thermal annealing. When subsequently photothermally heated in ambient oxygen, the resulting dehydrogenated graphene becomes reversibly hole-doped. Hydrogenated graphene had drawn interest for its predicted magnetism.[16] This particular reaction is also of technical interest since HSQ is a (negative-tone) electron beam resist used in patterning graphene nanoribbons.[17−19] Reactions of the HSQ-derived H atoms with the graphene basal planes should affect the electronic transport behavior of these nanostructured systems.

Results. ***Hydrogenation.*** Single or few-layer graphene samples were deposited by mechanically exfoliating kish graphite on Si wafer coated with a 300 nm thick layer of SiO_2.[20,21] The thickness and structural quality[22,23] of graphene samples were characterized by micro-Raman spectroscopy

* To whom correspondence should be addressed. E-mail: leb26@columbia.edu.
[†] Department of Chemistry.
[‡] Department of Applied Physics and Applied Mathematics.
[§] Departments of Physics and Electrical Engineering.
[||] Department of Physics.

10.1021/nl802940s CCC: $40.75
Published on Web 11/18/2008

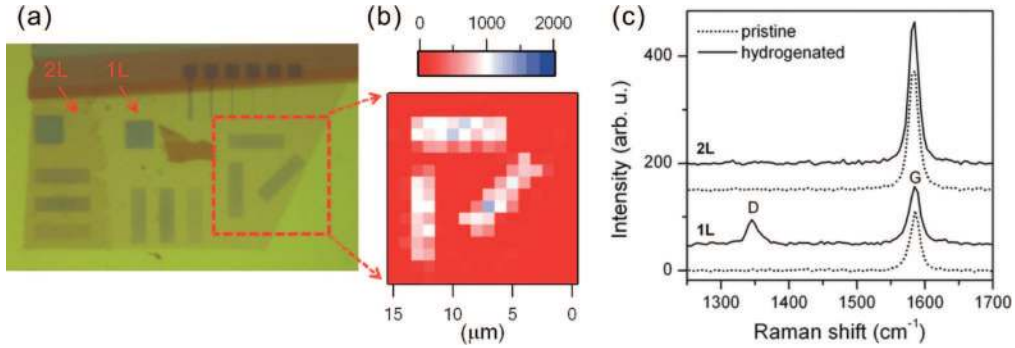

Figure 1. (a) Optical micrograph of e-beam patterned sample **II**, which contains 1 L, 2 L and thick sheets of graphene. The squares and rectangles are cross-linked HSQ etch masks. Noncross-linked HSQ has been removed by the developer. The 1 L area in the dashed square is $15 \times 15\ \mu m^2$ in size. (b) The D band intensity Raman map for the dashed square in (a). (c) Raman spectra taken at the center of 1 L and 2 L graphene squares (area: $4 \times 4\ \mu m^2$) shown in panel a before (dotted) and after (solid, displaced for clarity) hydrogenation. Data in panels b and c were obtained in ambient conditions with $\lambda_{exc} = 514.5$ nm. The employed laser power was 3 mW and focused onto a spot of $\sim 1\ \mu m$ in diameter. The integration time for each pixel was 20 s.

under ambient condition.[7] Hydrogen atoms were generated in situ by breaking Si−H bonds of HSQ in the course of e-beam lithography;[24] ~30 nm thick films of HSQ (Dow Corning, FOX) were coated on the graphene samples and irradiated with 30 keV electrons at various doses (0.5~8 mC/cm^2). Following development in tetramethylammonium hydroxide solution, some samples were treated with oxygen plasma to etch graphene areas not protected by the cross-linked HSQ film.[17] In one experiment (sample **I**), a Cr/Au electrode was connected to graphene in order to apply a back-gate voltage.

Sample **II** in Figure 1a shows several graphene pieces without electrode attachment. Squares and rectangles in single-layer (1 L) and double-layer (2 L) graphene areas are patterned by e-beam lithography. Raman spectra taken before HSQ e-beam patterning (pristine case in Figure 1c) show no detectible defect-related Raman D band (~1350 cm^{-1}), indicating that both the 1 L and 2 L sheets are initially free of defects. However, e-beam irradiation of 1 L graphene covered with HSQ induces a significant D band intensity, as readily seen in the Raman intensity map (Figure 1b). Calculations of the Raman response indicate that the D band is induced by local basal plane derivatization that creates sp^3 distortion.[25] Figure 1c shows Raman spectra taken at the center of the 1 L and 2 L squares. It is remarkable that identical e-beam doses generate virtually no D band on 2 L graphene, but a very prominent D band on 1 L graphene. While the defects are stable in ambient conditions at low laser intensities, intense laser excitation reduces the D band intensity as described below (for estimated temperature rise, see Supporting Information).

Pristine 1 L graphene without coating with an HSQ film showed negligible D band intensity after the same electron irradiation (see Supporting Information, Figure S1). Thus, the employed 30 keV electron dose does not directly create D band defects in the graphene lattice, which is consistent with prior studies on other carbon materials.[26,27] The electron beam causes Si−H bond scission in HSQ, thus initiating cross-linking.[24] We observe that the Si−H Raman band of HSQ[28] at 2265 cm^{-1} decreases by ~90% in intensity following the e-beam irradiation (Figure 2). Further, the D band intensity grows approximately linearly as e-beam exposure leads to hydrogen depletion in the HSQ, as indicated by the decreasing Si−H bond intensity. 2 L graphene is found to be much less reactive. The D band is seen only at very high e-beam dose and has ~60 times lower I_D/I_G (integrated intensity ratio of the D band to the G band) than 1 L graphene (Figure 2c) for the same dose. Given the same density of defects localized on the top graphene layer, the I_D/I_G ratio is expected to be smaller for 2 L than for 1 L samples because of the presence of an intact lower layer for 2 L samples. We estimate that the defect density of 1 L graphene is still at least 17 times higher than that for 2 L materials, based on the work by Z. Ni et al.[29] (see Supporting Information). H atoms should be the major mobile radical liberated by HSQ cross-linking: the Si−H bond is weaker than the Si−O bonds, and 2~3 bonds need to be broken simultaneously for Si, O, or SiO to be liberated from HSQ molecules.[28] We conclude that we observe the reaction of H atoms with the graphene basal plane.

The G band energy changes slightly following each step of treatment, as shown in Figure 3. Deposition of HSQ films and hydrogenation ($I_D/I_G \sim 1$) decrease the G band energy by <2 cm^{-1}. O_2 plasma treatment leads to an increase of <1 cm^{-1}. Physical contact of the ~30 nm HSQ film and subsequent solvent drying might lead to in-plane stress[29] thus affecting the G band energy. However, the reciprocal relation between the G band energy and its width (Figure 3) suggests that overall change is mainly driven by chemical doping; as demonstrated by electrical gating experiments, the concurrent upshift (downshift) and band narrowing (broadening) of the G band is explained by charge doping.[30,31] Because of nonadiabatic electron−phonon coupling, the G band shifts upward as the Fermi level is displaced from its neutrality point by doping. At the same time, the width of the G band decreases since Landau damping of the G phonon is not possible when the Fermi level is shifted by more than half of the G band energy from the neutrality point. When hydrogenated, graphene is expected to be electron doped since carbon is slightly more electronegative than hydrogen. This conclusion agrees with a recent DFT calculation[32] on the presence of a hydrogenation-induced Fermi level shift.

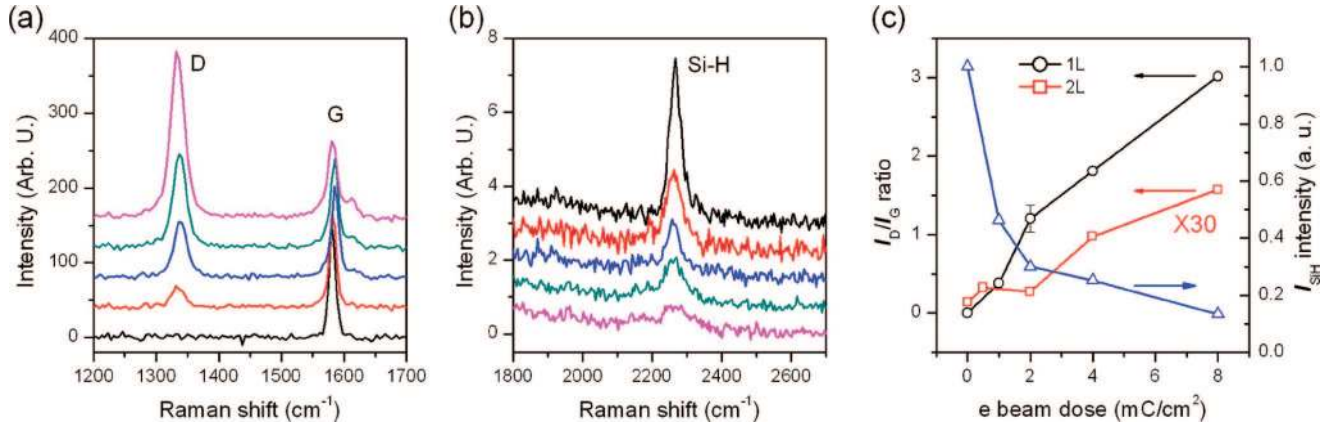

Figure 2. (a) Raman spectra of 1 L graphene sheets (sample **V**) at various stages of hydrogenation: the e-beam dose was 0, 1, 2, 4, and 8 mC/cm^2, respectively, from the bottom spectrum to the top one (displaced for clarity). (b) Raman spectra of HSQ films on SiO_2, irradiated with the same e-beam: the dose was 0, 1, 2, 4, and 8 mC/cm^2, respectively, from the top spectrum (displaced for clarity) to the bottom one. Each spectrum was obtained from a region of the HSQ film located within 10 μm from each of the above graphene sheets. (c) Integrated intensity ratio of the D band to G band (I_D/I_G) as a function of e-beam dose: 1 L (circles) and 2 L (squares) graphene. Triangles represent the Si−H band intensity as a function of e-beam dosage. All spectra were obtained in ambient conditions with the 514.5 nm excitation laser focused to a spot size of ~1 μm diameter. The laser power was 0.1 and 3 mW for panels a and b, respectively.

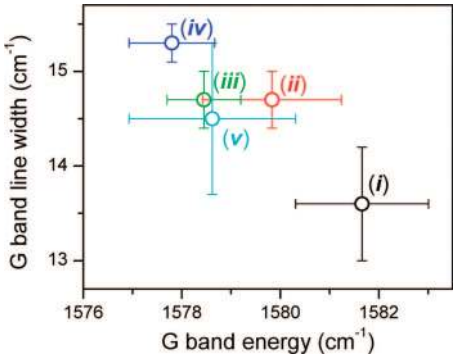

Figure 3. G band line width vs energy, obtained for sample **III** following each treatment step: (i) no treatment-pristine graphene, (ii) after HSQ film deposition, (iii) after hydrogenation (e-beam dose: 0.5 mC/cm^2), (iv) after additional hydrogenation (accumulated e-beam dose: 1.0 mC/cm^2), and (v) after oxygen plasma treatment. The error bars represent standard deviations for 10 spots measured in one graphene sample. All data were obtained in ambient conditions. The excitation laser operated at a wavelength of λ_{exc} = 514.5 nm and a power of 3 mW was used in a spot size of ~1 μm diameter. The line width includes an instrument response function of 6.0 cm^{-1}.

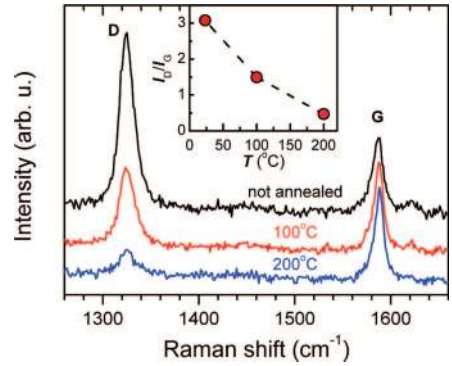

Figure 4. Raman spectra of hydrogenated 1 L graphene (sample **I**) taken before and after oven annealing for 1 h at 100 °C (in air) and 200 °C (in Ar). The inset shows the ratio of I_D/I_G as a function of the annealing temperature. The spectra were obtained under ambient conditions. The Raman pump laser was operated at a wavelength of λ_{exc} = 632.8 nm with a power of 4 mW focused to a spot of ~2 μm diameter.

Electron doping is also consistent with the observed red shift of the G band upon hydrogenation, since initial graphene on silicon dioxide is lightly hole-doped from the environment.[20]

The reaction of H atoms with multilayer graphite has previously been studied in detail.[33−35] The binding energy of a single H atom is low (~0.7 eV). Isolated adsorbed H atoms (H_{ad}) show a relatively small activation energy for desorption (~0.9 eV) and are not stable at room temperature.[33−35] Para or ortho H_{ad} pairs in one benzene ring form at higher coverages. Pairs are more strongly bound and have a significantly larger activation energy for recombinative desorption as H_2.[35] We do not know if we are observing single or paired H_{ad} on our graphene samples.

On graphite, H adsorption is reversible; thermal desorption spectra have one major desorption peak at ~200 °C and a minor one at ~290 °C.[36] In a combined STM study, it has been shown that annealing at 423 °C completely removes adsorbed H atoms, restoring the original crystalline lattice without vacancies. In Figure 4, oven annealing of hydrogenated 1 L graphene also shows partial reversibility. After annealing, the Raman D band decreases drastically in intensity relative to the G band. The I_D/I_G ratio decreases by more than a factor of 6 when annealed in Ar at 200 °C (inset of Figure 4). This comparison also supports our assignment of the D band to the influence of hydrogenation.

Figure 4 shows that the defects induced by hydrogenation can be thermally healed to a significant extent, largely restoring the original graphene lattice. Intense focused laser radiation also induces a similar effect as shown in Figure 5c. During repeated Raman measurements, the I_D/I_G ratio gradually decreases because of photothermal desorption of H. The temperature of graphene induced by photothermal heating in Figure 5 is estimated to be ~60 °C based on the temperature coefficient of the G band energy[37] (see Sup-

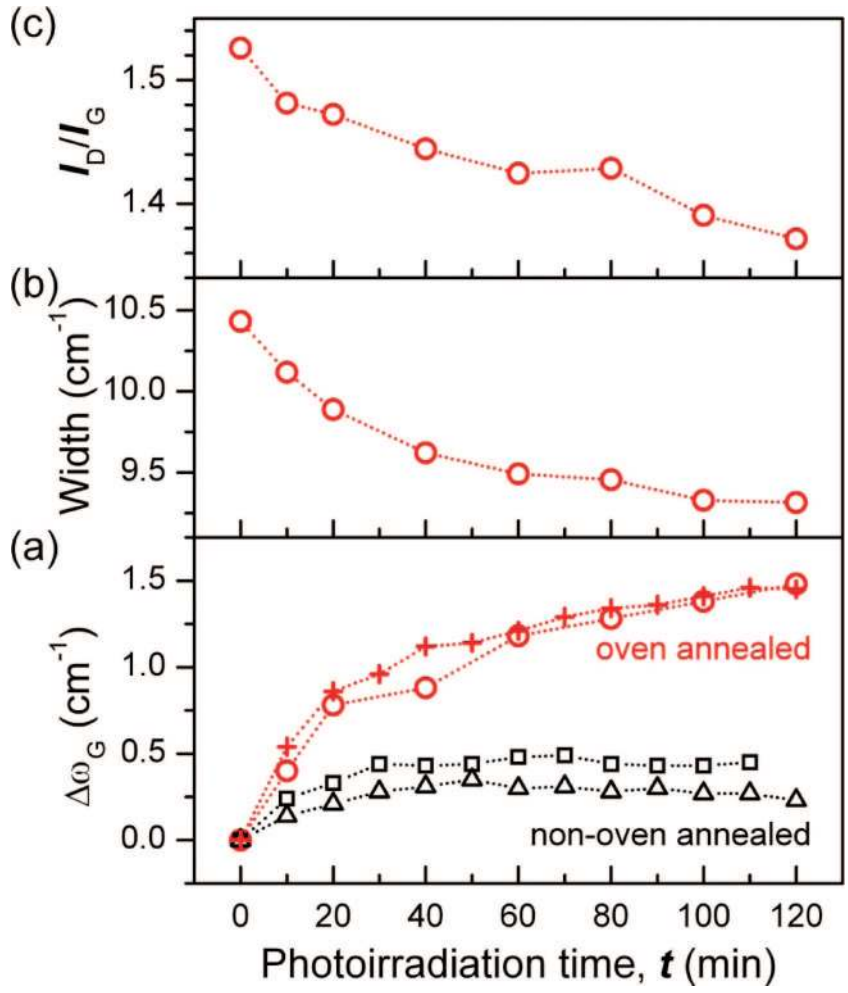

Figure 5. Effects of prolonged photoirradiation in O_2 atmosphere on 1 L graphene Raman spectra: (a) G band energy change, $\Delta\omega_G = \omega_G(t) - \omega_G(t = 0)$, (b) G band line width, and (c) I_D/I_G as a function of photoirradiation time (t). The history of the samples is as follows. Circles (sample **I**) hydrogenated (0.5 mC/cm^2) followed by oven annealing in air at 100 °C; crosses (sample **VI**) hydrogenated (0.5 mC/cm^2) followed by oven annealing in Ar at 100 °C; triangles (sample **VI**) hydrogenated (0.5 mC/cm^2) but not oven annealed; squares (sample **V**) HSQ-coated but non-hydrogenated and nonoven annealed. Two micrometer spots of each sample were continuously irradiated with a 632.8 nm laser (4 mW) for 120 min during the course of the Raman measurements. The line width includes an instrument response function of 3.7 cm^{-1}.

porting Information). The controllable hydrogenation with the high spatial resolution of e-beam lithography and reversible dehydrogenation may find application in patterning graphene into semiconducting or insulating nanodomains. This approach could also be applied to carbon nanotubes and other graphitic materials.

Activation for Subsequent Reaction. After thermal annealing, the Raman spectrum of the dehydrogenated graphene is similar to the initial Raman spectrum, except for a residual D band. Nevertheless, after oven annealing the sample is "activated"; it shows enhanced chemical doping when photothermally heated in an oxygen atmosphere. In Figure 5a, the G band energy is plotted as a function of photoirradiation time. While nonoven annealed graphene (hydrogenated or non-hydrogenated) shows less than a 0.5 cm^{-1} increase, the graphene G band blue-shifts by 1.5 cm^{-1} after oven annealed in air or Ar at 100 °C. The simultaneous G band narrowing in Figure 5b suggests that charge doping occurs. Notably, the blue shift is mostly attributed to chemical doping caused by molecular oxygen; the G band energy of the photothermally heated graphene decreases (increases) in Ar (O_2) atmosphere with concurrent line width broadening (narrowing) (see Supporting Information, Figure S2 and S3).

To determine the polarity of charge doped by O_2, we titrated with electrically induced charge. Graphene connected to an external electrode forms a capacitor with the Si back gate; it accumulates electrons (holes) by applying positive (negative) gate voltage.[30,31] Figure 6a,b presents the G band energy and line width, respectively, measured for the dehydrogenated graphene (as in Figure 3) as a function of gate voltage (V_G) in both Ar and O_2 flow. (For spectra, see Supporting Information, Figure S4). In Ar, the G band energy has a minimum at $V_G \approx +5$ V, which indicates that the annealed graphene is barely doped in the Ar environment. However, in O_2 the G band energy minimum is located at $V_G > +50$ V, which indicates that the annealed graphene is heavily doped with holes ($>4 \times 10^{12}$ holes/cm^2), requiring additional electrons for compensation. The line width shown in Figure 6b correlates well with the G band energy, as

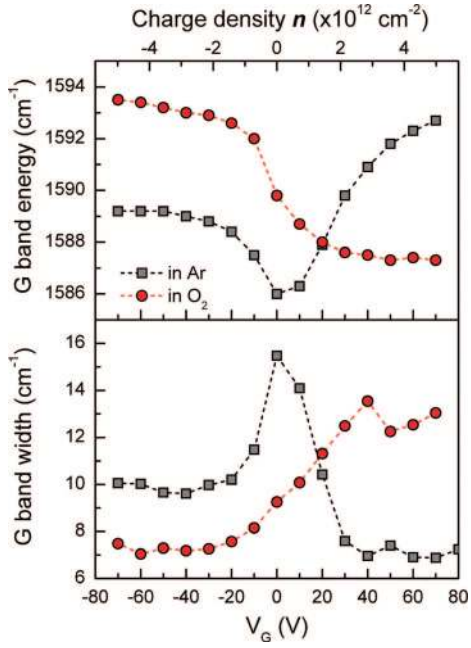

Figure 6. G band energy (upper) and line width (lower) of 1 L graphene (sample **I**), obtained as a function of back-gate voltage (V_G) in Ar and O_2. The graphene sample was dehydrogenated at 100 °C in air in the oven, followed by further photothermal heating. The charge density (n) of upper x-axis refers to the number density of electrons in graphene induced by the electrical gating. According to ref 30, $n = C_G V_G/e$, where C_G is 115 aF/μm^2. The line width includes an instrument response function of 3.7 cm^{-1}.

discussed earlier. Thus, we conclude that molecular oxygen binds reversibly to oven-annealed activated graphene, leading to hole doping at room temperature.

Discussion. ***Hydrogenation.*** Near room temperature, H atoms are more reactive with 1 L than 2 L graphene. The enhanced reactivity of single-layer graphene was also seen earlier in oxidative etching at higher temperatures.[7] This suggests that 1 L graphene shows a distortion, or degree of freedom, not present in 2 L. 1 L graphene does not have multilayer π-stacking, which favors a flat structure and is known to increase reaction activation barriers.[6] 1 L graphene has significant ripples both when free-standing[8] and when supported on SiO_2 substrates.[11,12,38] The ripples were found to decrease with increasing thickness of the graphene samples.[8,38] Such out-of-plane ripples induce some sp^3 hybridization in otherwise sp^2-hybridized carbons. A recent Monte Carlo simulation confirming energetically stable ripples in free-standing graphene also concluded that the C−C bond length of rippled graphene has a significantly broader variation than that of flat graphene.[9] These factors naturally explain the enhanced reactivity of 1 L graphene.

Although the density of the defects has not been determined experimentally, an order-of-magnitude estimation can be made based on simulations of the Raman spectra of hydroxylated graphene.[25] For evenly distributed 1,2-hydroxyl pairs with an OH density of 4.8×10^{14} /cm^2 (0.13 ML), the D band is predicted to be as intense as G band. Because the I_D/I_G ratio of the hydrogenated graphene in Figure 2a (2 mC/cm^2) is roughly unity, the H defect number density can be estimated to be $\sim 5 \times 10^{14}$ /cm^2. Given the average HSQ film thickness of 30 nm, density[39] of $\sim$1.3 g/cm^3, and molecular weight of 424 as $H_8Si_8O_{12}$, the maximum integrated H atom flux available is 4.4×10^{16} /cm^2 (equivalent to $\sim$10 ML). This gives $\sim$0.03 for net sticking probability (S) of H atom on 1 L graphene at 300 K, assuming that $\sim$70% of Si−H bonds are dissociated (Figure 2c) and that half of the liberated H atoms reach graphene surface. We neglect here H recombination or other loss mechanisms; such processes would make S higher.

On the basis of the G band energy change, the amount of charge transferred from a single hydrogen atom can be estimated. The G band energy shift of ≤ 2 cm^{-1} (Figure 3) caused by the hydrogenation giving $I_D/I_G \sim 1$ (Supporting Information, Figure S1b) corresponds roughly to a change in charge density of $\sim 1.3 \times 10^{12}$ e/cm^2.[30] Assuming the number density of H defects is $\sim 5 \times 10^{14}$ /cm^2 (0.13 ML), $\sim 0.003e$ charge is donated by each chemisorbed H atom. Compared to chemical doping by weakly interacting molecules such as water, NH_3, CO, and NO,[40] the estimated charge transfer is several times lower. This appears reasonable considering the largely nonpolar nature of C−H bonds. Controllable chemical doping by forming covalent bonds of varying polarity can be exploited to modify the electronic properties of graphene for possible device applications.

Activation for Subsequent Reaction. We find that graphene oven annealed at 100 °C is more reactive than pristine graphene. Recently, Li et al. observed that graphene annealed at >250 °C is activated and unlike the initial pristine graphene reversibly binds oxygen molecules under ambient. We infer that thermal or photothermal annealing generates at present unknown structural changes. Molecular oxygen in its excited singlet state is known to form endoperoxides with hundreds of aromatic compounds.[41] Because of the sp^3 character of carbon atoms connected to O_2 in endoperoxides, strained π-systems have much higher affinity to O_2 than do planar ones. Owing to its severe strain as well as extended conjugation, helianthrene is known to bind even ground-state triplet O_2 to form endoperoxides.[42] Carbon nanotubes, systematically strained by curvature yet showing no D band, also bind O_2 to form endoperoxides.[43]

Thermal annealing may remove water and extraneous organic matter initially present between graphene layers and the substrate SiO_2. Graphene annealed in direct contact with atomically rough SiO_2 may further deform. Graphene on SiO_2 is 60% smoother in height variation than the bare SiO_2 surface,[12] which implies that the annealed graphene sheet has deformed in response to the substrate.[7] The substrate-mediated thermal activation is thought to generate O_2-binding sites with a high degree of out-of-plane deformation. Compared to graphene annealed at >250 °C, the doping level of the photothermally heated graphene is much lower, which implies that further activated deformation can occur. We doubt that activation represents vacancy formation; oxygen would bind strongly and irreversibly to a vacancy cite.[44]

In conclusion, we have shown that 1 L graphene can be more easily hydrogenated than 2 L graphene near room temperature. This enhanced reactivity is attributed to the lack of π-stacking and/or out-of-plane deformation needed to

stabilize the transition state of the hydrogenation reaction. The hydrogenated graphene can be restored by thermally desorbing bound hydrogen atoms. Dehydrogenated graphene on SiO_2 is activated and exhibits enhanced chemical doping caused by oxygen molecules when photothermally heated. The bound oxygen molecules lead to reversible hole doping of graphene.

Acknowledgment. This work was funded by the Department of Energy under Grants DE-FG02-03ER15463 (T.F.H) and DE-FG02-98ER14861 (L.E.B) and by National Science Foundation under No. DMR-0349232 (P.K.). We acknowledge financial support from the Nanoscale Science and Engineering Initiative of the National Science Foundation under NSF Award No. CHE-06-41523 by the Nanoelectronics Research Initiative (NRI) of the Semiconductor Research Corporation and by the New York State Office of Science, Technology, and Academic Research (NYSTAR). J.M. acknowledges support from the Alexander von Humboldt foundation.

Supporting Information Available: The dependence of the D band sensitivity on graphene thickness, photothermally induced reversible O_2 binding on preannealed graphene, temperature of graphene under photothermal heating, effects of e-beam irradiation on the Raman spectra of bare graphene compared to HSQ-covered graphene, raw Raman scattering data for Figure 6. This material is available free of charge via the Internet at http://pubs.acs.org.

References

(1) Bolotin, K. I.; Sikes, K. J.; Jiang, Z.; Fundenberg, G.; Hone, J.; Kim, P.; Stormer, H. L. *Solid State Commun.* **2008**, *146*, 351.
(2) Geim, A. K.; Novoselov, K. S. *Nat. Mater.* **2007**, *6*, 183–191.
(3) Stankovich, S.; Dikin, D. A.; Dommett, G. H. B.; Kohlhaas, K. M.; Zimney, E. J.; Stach, E. A.; Piner, R. D.; Nguyen, S. T.; Ruoff, R. S. *Nature* **2006**, *442*, 282–286.
(4) Dikin, D. A.; Stankovich, S.; Zimney, E. J.; Piner, R. D.; Dommett, G. H. B.; Evmenenko, G.; Nguyen, S. T.; Ruoff, R. S. *Nature* **2007**, *448*, 457–460.
(5) Ruoff, R. *Nat. Nanotechnol.* **2008**, *3*, 10.
(6) Xu, S. C.; Irle, S.; Musave, D. G.; Lin, M. C. *J. Phys. Chem. C* **2007**, *111*, 1355.
(7) Liu, L.; Ryu, S.; Tomasik, M. R.; Stolyarova, E.; Jung, N.; Hybertsen, M. S.; Steigerwald, M. L.; Brus, L. E.; Flynn, G. W. *Nano Lett.* **2008**, *8*, 1965.
(8) Meyer, J. C.; Geim, A. K.; Katsnelson, M. I.; Novoselov, K. S.; Booth, T. J.; Roth, S. *Nature* **2007**, *446*, 60–63.
(9) Fasolino, A.; Los, J. H.; Katsnelson, M. I. *Nat. Mater.* **2007**, *6*, 858–861.
(10) Lee, C.; Wei, X.; Kysar, J. W.; Hone, J. *Science* **2008**, *321*, 385.
(11) Stolyarova, E.; Rim, K. T.; Ryu, S.; Maultzsch, J.; Kim, P.; Brus, L. E.; Heinz, T. F.; Hybertsen, M. S.; Flynn, G. W. *Proc. Natl. Acad. Sci. U.S.A.* **2007**, *104*, 9209–9212.
(12) Ishigami, M.; Chen, J. H.; Cullen, W. G.; Fuhrer, M. S.; Williams, E. D. *Nano Lett.* **2007**, *7*, 1643–1648.
(13) Ruffieux, P.; Gröning, O.; Bielmann, M.; Mauron, P.; Schlapbach, N/A; Gröning, P. *Phys. Rev. B* **2002**, *66*, 245416.
(14) Niyogi, S.; Hamon, M. A.; Hu, H.; Zhao, B.; Bhowmik, P.; Sen, R.; Itkis, M. E.; Haddon, R. C. *Acc. Chem. Res.* **2002**, *35*, 1105–1113.
(15) Ferrari, A. C. *Solid State Commun.* **2007**, *143*, 47–57.
(16) Yazyev, O. V.; Helm, L. *Phys. Rev. B* **2007**, *75*, 125408.
(17) Han, M. Y.; Oezyilmaz, B.; Zhang, Y.; Kim, P. *Phys. Rev. Lett.* **2007**, *98*, 206805/1–206805/4.
(18) Chen, Z.; Lin, Y.-M.; Rooks, M. J.; Avouris, P. *Physica E* **2007**, *40*, 228.
(19) Lin, Y.-M.; Perebeinos, V.; Chen, Z.; Avouris, P. http://arxiv.org/abs/0805.0035v2 (accessed November 14, 2008).
(20) Novoselov, K. S.; Geim, A. K.; Morozov, S. V.; Jiang, D.; Zhang, Y.; Dubonos, S. V.; Grigorieva, I. V.; Firsov, A. A. *Science* **2004**, *306*, 666–9.
(21) Zhang, Y.; Tan, Y.-W.; Stormer, H. L.; Kim, P. *Nature* **2005**, *438*, 201–204.
(22) Ferrari, A. C.; Meyer, J. C.; Scardaci, V.; Casiraghi, C.; Lazzeri, M.; Mauri, F.; Piscanec, S.; Jiang, D.; Novoselov, K. S.; Roth, S.; Geim, A. K. *Phys. Rev. Lett.* **2006**, *97*, 187401/1–187401/4.
(23) Ferrari, A. C.; Robertson, J. *Phys. Rev. B* **2000**, *61*, 14095–14107.
(24) Namatsu, H.; Takahashi, Y.; Yamazaki, K.; Yamaguchi, T.; Nagase, M.; Kurihara, K. *J. Vac. Sci. Technol., B* **1998**, *16*, 69.
(25) Kudin, K. N.; Ozbas, B.; Schniepp, H. C.; Prud'homme, R. K.; Aksay, I. A.; Car, R. *Nano Lett.* **2008**, *8*, 36–41.
(26) Smith, B. W.; Luzzi, D. E. *J. Appl. Phys.* **2001**, *90*, 3509.
(27) Krasheninnikov, A. V.; Banhart, F. *Nat. Mater.* **2007**, *6*, 723.
(28) Bornhauser, P.; Calzaferri, G. *J. Phys. Chem.* **1996**, *100*, 2305.
(29) Ni, Z. H.; Wang, H. M.; Ma, Y.; Kasim, J.; Wu, Y. H.; Shen, Z. X. *ACS Nano* **2008**, *2*, 1033.
(30) Yan, J.; Zhang, Y.; Kim, P.; Pinczuk, A. *Phys. Rev. Lett.* **2007**, *98*, 166802.
(31) Pisana, S.; Lazzeri, M.; Casiraghi, C.; Novoselov, K. S.; Geim, A. K.; Ferrari, A. C.; Mauri, F. *Nat. Mater.* **2007**, *6*, 198–201.
(32) Yazyev, O. V.; Helm, L. *Phys. Rev. B* **2007**, *75*, 125408.
(33) Sha, X.; Jackson, B. *Surf. Sci.* **2002**, *496*, 318.
(34) Jeloaica, L.; Sidis, V. *Chem. Phys. Lett.* **1999**, *300*, 157.
(35) Hornekaer, L.; Sljivancanin, Z.; Xu, W.; Otero, R.; Rauls, E.; Stensgaard, I.; Laegsgaard, E.; Hammer, B.; Besenbacher, F. *Phys. Rev. Lett.* **2006**, *96*, 156104.
(36) Zecho, T.; Gü ttler, A.; Sha, X.; Jackson, B.; Kü ppers, J. *J. Chem. Phys.* **2002**, *117*, 8486.
(37) Calizo, I.; Balandin, A. A.; Bao, W.; Miao, F.; Lau, C. N. *Nano Lett.* **2007**, *7*, 2645.
(38) Knox, K. R.; Wang, S.; Morgante, A.; Cvetko, D.; Locatelli, A.; Mentes, T. O.; Niño, M. A.; Kim, P. R. M. O., Jr. http://arxiv.org/abs/0806.0355v1 (accessed November 14, 2008).
(39) Liou, H.-C.; Dehate, E.; Duel, J.; Dall, F. *Mater. Res. Soc. Symp. Proc.* **2000**, *612*, D5–12.
(40) Leenaerts, O.; Partoens, B.; Peeters, F. M. *Phys. Rev. B* **2008**, *77*, 125416.
(41) Aubry, J.-M.; Pierlot, C.; Rigaudy, J.; Schmidt, R. *Acc. Chem. Res.* **2003**, *36*, 668.
(42) Seip, M.; Brauer, H. D. *J. Am. Chem. Soc.* **1992**, *114*, 4486.
(43) Dukovic, G.; White, B.; Zhou, Z.; Wang, F.; Jockusch, S.; Heinz, T.; Turro, N.; Friesner, R.; Brus, L. *J. Am. Chem. Soc.* **2004**, *126*, 15269.
(44) Lee, S. M.; Lee, Y. H.; Hwang, Y. G.; Hahn, J. R.; Kang, H. *Phys. Rev. Lett.* **1999**, *82*, 217–220.

NL802940S